INTERNATIONAL JOURNAL FOR NUMERICAL METHODS IN FLUIDS, VOL. 4, 291–302 (1984)

FINITE ELEMENT METHOD FOR UNSTEADY MHD FLOW THROUGH PIPES WITH ARBITRARY WALL CONDUCTIVITY

BANI SINGH

Department of Mathematics, University of Roorkee, Roorkee, U.P., India

JIA LAL

Roorkee University Regional Computer Centre, Roorkee, U.P., India

SUMMARY

A finite element method is given to obtain the numerical solution of the coupled equations in velocity and magnetic field for unsteady MHD flow through a pipe having arbitrarily conducting walls. Pipes of rectangular, circular and triangular sections have been taken for illustration. Computations have been carried out for different Hartmann numbers and wall conductivity at various time levels. It is found that if the wall conductivity increases, the flux through a section decreases. The same is the effect of increasing the Hartmann number. It is also observed that the steady state is approached at a faster rate for larger Hartmann numbers or larger wall conductivity. Selected graphs are given showing the behaviour of velocity, induced magnetic field and flux across a section.

KEY WORDS Finite Elements MHD Flows

INTRODUCTION

The study of the flow of conducting fluids in the presence of transverse magnetic fields has attracted attention owing to its applications in such diversified fields as astrophysics, geology, power generation, flowmetry, thermonuclear reactor technology, etc. it is, therefore, not surprising that a lot of theoretical and experimental work has been carried out in this direction during the last twenty years. In general, the problems of MHD flow are extremely complex, and analytic solutions are out of the question. However, in some simple cases, exact solutions have been found. The axial flow through a straight pipe in the presence of a uniform transverse magnetic field is one such example.[1–10] In most of these cases, the walls have been taken as non-conducting, although some authors have also considered perfectly conducting walls or a combination of non-conducting and perfectly conducting walls. The geometry of the section has been taken as a circle, rectangle, ellipse, sector, etc. To deal with more intractable cases, numerical methods are the only alternative.

The authors have applied numerical methods such as FDM and FEM to steady MHD channel flow problems with non-conducting and arbitrarily conducting walls.[10–15] Although steady flows have been studied extensively, only a few papers have appeared on unsteady flows. Gupta and Singh[16,17] obtained exact solutions for unsteady flows in some special cases. Gupta[18] has obtained solutions for unsteady flow with small Hartmann number. Gupta and Mittal[19] gave exact solutions for unsteady flow through a pipe with section as an annular region. The authors have applied the Crank–Nicolson and alternating direction implicit

0271–2091/84/030291–12$01.20

Received 5 July 1982
Revised 10 January 1983

methods to obtain numerical solution of unsteady flow through a rectangular pipe.[20] Recently, Wu[21] has applied the finite element method to unsteady flow between two infinite parallel planes. However, his assumptions are not always valid in practice.

In all the references cited above for unsteady flows, the walls are taken non-conducting. When the wall conductivity is different from zero, the problem is much more difficult. The present paper deals with the application of the finite element method to unsteady MHD flow through a straight pipe of infinite length with section of an arbitrary shape and arbitrary wall conductivity. The authors have not come across even a single paper dealing with this case.

First of all, the time variable has been eliminated by integration. For the resulting system of equations, a variational principle has been found. To this the Ritz FEM is then applied. Calculations are carried out step by step in the time direction till the steady state is reached. Pipes with section as a rectangle, a circle and an equilateral triangle are taken for illustration. Computations are carried out for various Hartmann numbers and wall conductivity at various time levels. It is found that if the wall conductivity and/or Hartmann number are increased, the flux through a section is reduced and the steady state is approached at a faster rate.

BASIC EQUATIONS

Let the co-ordinate system be chosen such that the X-axis is along the applied magnetic field B_0, the Y-axis is perpendicular to it and lying in a section, and the Z-axis is along the axial direction in which the flow is taking place. Then for viscous and incompressible fluid, the governing equations in the MKS system are[16,17]

$$\left.\begin{aligned} \rho\frac{\partial V_Z}{\partial T} &= -\frac{\partial p}{\partial Z}+\eta\nabla^2 V_Z+\frac{B_0}{\mu_0}\frac{\partial B_Z}{\partial X} \\ \frac{\partial B_Z}{\partial T} &= (\mu_0\sigma)^{-1}\nabla^2 B_Z+B_0\frac{\partial V_Z}{\partial X} \end{aligned}\right\} \text{ in the flow region}$$

where ρ, η, σ are the density, coefficient of viscosity and electric conductivity of the fluid. $V_Z(X, Y, T)$ and $B_Z(X, Y, T)$ are the axial velocity and the induced magnetic field, p is the pressure, T the time and μ_0 is a constant which has the value $4\pi\times 10^{-7}$ in the MKS system. ∇^2 is the two-dimensional Laplacian operator in the XY-plane. The boundary conditions on V_Z and B_Z are

$$V_Z = 0, \quad \frac{\partial B_Z}{\partial N}+\frac{\sigma}{\sigma'}\frac{B_Z}{h}=0 \quad \text{on the boundary}$$

where N is the outward normal to the boundary of the section, σ' is the electric conductivity of the walls and h is the thickness of the walls which is taken to be small. The first condition is the no-slip condition, the second has been taken from Reference 4. The initial conditions depend upon how the motion starts initialty. For example, if the motion starts from rest, the initial conditions become

$$V_Z = 0, \qquad B_Z = 0 \quad \text{at time} \quad T = 0$$

Let us introduce the following non-dimensional variables and parameters:

$$V = V_Z/V_0, \qquad V_0 = Ka^2/\eta, \qquad B = B_Z/V_0\mu_0\sqrt{(\sigma\eta)}$$
$$x = X/a, \qquad y = Y/a, \qquad M^2 = B_0^2a^2\sigma/\eta, \qquad \lambda = \sigma a/\sigma' h$$
$$R = \rho a^2 V_0/\eta, \qquad R_m = V_0 a\mu_0\sigma, \qquad T = ta/V_0, \qquad f(t) = F(at/V_0)$$

where M, R, R_m are the Hartmann number, Reynolds number and magnetic Reynolds number, respectively. The pressure gradient $\partial p/\partial Z = -KF(T)$, where $F(T)$ is a known function of time and a is the characteristic length. Then the governing equations, the boundary conditions and the initial conditions are reduced to the following non-dimensional form:

$$\left.\begin{aligned} \nabla^2 V + M\frac{\partial B}{\partial x} &= -f(t) + R\frac{\partial V}{\partial t} \\ \nabla^2 B + M\frac{\partial V}{\partial x} &= R_m\frac{\partial B}{\partial t} \end{aligned}\right\} \text{ in } D\times[0,\infty], \tag{1,2}$$

$$V = 0, \quad \text{on } \partial D, \quad t \geq 0 \tag{3}$$

$$\frac{\partial B}{\partial n} + \lambda B = 0, \quad \text{on } \partial D, \quad t \geq 0 \tag{4}$$

$$V(x, y, 0) = 0, \quad \text{in } D \tag{5}$$

$$B(x, y, 0) = 0, \quad \text{in } D \tag{6}$$

where D represents the section of the pipe in non-dimensional form with ∂D as the boundary, n is the outward normal and ∇^2 the two-dimensional Laplacian operator in the xy-plane. Notice that for non-conducting walls $\sigma' = 0$. So $\lambda = \infty$ and the boundary condition on B becomes $B = 0$. In the other extreme case when the walls are perfectly conducting $\sigma' = \infty$ or $\lambda = 0$ and the boundary condition becomes $\partial B/\partial n = 0$.

As already pointed out, the exact solution of the above equations is not possible in general. However, in some special cases with $\lambda = \infty$, $R = R_m$, the exact solutions have been obtained.[16,17,19] These are too complicated to be given here. Computationally, these solutions are not of much utility as the series summations are quite time consuming and at each point the series have to be summed up separately. Keeping these difficulties in mind, Singh and Lal[20] applied the Crank–Nicolson and ADI methods for a rectangular pipe with non-conducting walls. Although the ADI method proves to be quite efficient for the rectangular geometry, for an arbitrary boundary it cannot compete with the FEM.

VARIATIONAL PRINCIPLE

In order to apply FEM, we have first integrated (1) and (2) with respect to time and then found a variational principle for the resulting system. This alternative to the usual procedure leads to a simpler variational principle and has been used successfully by Verruijt[22] for solving a two-dimensional diffusion equation.

So, integrating (1) and (2) with respect to t from t^n to t^{n+1} and assuming linear variation of V, B and $f(t)$ in $[t^n, t^{n+1}]$, where $\Delta t^n = t^{n+1} - t^n$ is small, we finally get

$$\left.\begin{aligned} \nabla^2 V^* + M\frac{\partial B^*}{\partial x} &= -f^* + \beta^n(V^* - V^n) \\ \nabla^2 B^* + M\frac{\partial V^*}{\partial x} &= \gamma^n(B^* - B^n) \end{aligned}\right\} \text{ in } D \tag{7,8}$$

where V^*, B^*, f^* are the average values of V, B and f in $[t^n, t^{n+1}]$ and

$$\beta^n = 2R/\Delta t^n, \qquad \gamma^n = 2R_m/\Delta t^n \tag{9}$$

The boundary conditions on V^* and B^* become

$$\left.\begin{aligned} V^* &= 0 \\ \frac{\partial B^*}{\partial n} + \lambda B^* &= 0 \end{aligned}\right\} \text{ on } \partial D \tag{10, 11}$$

Assuming that V^n, B^n at time t^n are known, the problem now reduces to solving (7) and (8) subject to boundary conditions (10) and (11). After knowing V^* and B^*, the values at time t^{n+1} are calculated from

$$V^{n+1} = 2V^* - V^n, \qquad B^{n+1} = 2B^* - B^n \tag{12}$$

Since the values V^0, B^0 at time $t^0 = 0$ are known from the initial conditions, we can adopt the above procedure to find values at t^1, t^2, t^3, and so on.

After some tricky and lengthy calculations, it is found that the problem of solving (7) and (8) subject to (10) and (11) is equivalent to extremizing the functional

$$I = \iint_D \left[V^* g^n - \tfrac{1}{2}\beta^n (V^*)^2 - \tfrac{1}{2}(\nabla V^*)^2 - h^n B^* + \tfrac{1}{2}\gamma^n (B^*)^2 + \tfrac{1}{2}(\nabla B^*)^2 + \alpha\left(V^* \frac{\partial B^*}{\partial x} - B^* \frac{\partial V^*}{\partial x} \right) \right] dD + \tfrac{1}{2}\lambda \int_{\partial D} (B^*)^2 \, ds \tag{13}$$

where,

$$\alpha = M/2, \qquad g^n(x, y) = f^* + \beta^n V^n(x, y), \qquad h^n(x, y) = \gamma^n B^n(x, y) \tag{14}$$

FINITE ELEMENT FORMULATION

Let us divide the region D into E linear triangular elements which lead to, say, a total number of m nodes, out of which m_0 are internal and the remaining $m - m_0$ are the boundary nodes. Over the closed domain $\bar{D} = D \cup \partial D$, we approximate V^* and B^* by

$$V^*(x, y) = \sum_{q=1}^{m} N_q(x, y) V_q^* \tag{15}$$

$$B^*(x, y) = \sum_{q=1}^{m} N_q(x, y) B_q^* \tag{16}$$

where V_q^*, B_q^* are the nodal values and $N_q(x, y)$ are the shape functions. Notice that V_q^* vanishes for $q = (m_0 + 1)(1)m$ due to the boundary conditions. So the unknowns are V_q^*, $q = 1(1)m_0$ and B_q^*, $q = 1(1)m$, i.e. in all $m + m_0$ in number. For the non-conducting walls B_q^*, $q = (m_0 + 1)(1)m$ are also zero. So in that case the total number of unknowns becomes $2m_0$.

Substituting (15), (16) in (13) and extremizing I with respect to the unknown nodal values, i.e. using

$$\partial I / \partial V_q^* = 0, \qquad q = 1(1)m_0; \qquad \partial I / \partial B_q^* = 0, \qquad q = 1(1)m$$

we finally get the following system of equations

$$\sum_{q=1}^{m_0} (a_{pq} + \beta^2 b_{pq}) V_q^* + \alpha \sum_{q=1}^{m} c_{pq} B_q^* = r_p^n, \qquad p = 1(1)m_0 \tag{17}$$

$$\sum_{q=1}^{m} (a_{pq} + \gamma^n b_{pq} + \lambda d_{pq}) B_q^* + \alpha \sum_{q=1}^{m_0} c_{pq} V_q^* = s_p^n, \qquad p = 1(1)m_0 \tag{18}$$

where a_{pq}, b_{pq}, c_{pq}, d_{pq}, r_p^n, s_p^n are given by

$$\left.\begin{aligned} a_{pq} &= \iint_D \left[\frac{\partial N_p}{\partial x}\frac{\partial N_q}{\partial x} + \frac{\partial N_p}{\partial y}\frac{\partial N_q}{\partial y}\right] \mathrm{d}D \\ b_{pq} &= \iint_D N_p N_q \, \mathrm{d}D \\ c_{pq} &= \iint_D \left[\frac{\partial N_p}{\partial x} N_q - \frac{\partial N_q}{\partial x} N_p\right] \mathrm{d}D \\ d_{pq} &= \int_{\partial D} N_p N_q \, \mathrm{d}s \\ r_p^n &= \iint_D g^n N_p \, \mathrm{d}D \\ s_p^n &= \iint_D h^n N_p \, \mathrm{d}D \end{aligned}\right\} \tag{19}$$

Notice that the matrices $[a_{pq}]$, $[b_{pq}]$, $[c_{pq}]$ and $[d_{pq}]$ are independent of n. So they can be computed only once and used for all steps in the time direction. The contributions to the first three matrices from a typical element e with nodes i, j, k are given by

$$\left.\begin{aligned} a_{pq}^e &= (b_p^e b_q^e + c_p^e c_q^e)\Delta^e = a_{qp}^e \\ b_{pq}^e &= (1 + \delta_{pq})\,\Delta^e/12 = b_{qp} \\ c_{pq}^e &= (b_p^e - b_q^e)\,\Delta^e/3 = -c_{qp} \end{aligned}\right\} \; p.\, q = i, j, k \tag{20}$$

where Δ^e is the area of the element e and

$$b_i^e = (y_j - y_k)/2\,\Delta^e, \qquad c_i^e = (x_k - x_y)/2\,\Delta^e, \text{ etc.}$$

with (x_i, y_i) as the co-ordinates of the node i. The contribution to $[d_{pq}]$ comes only from those elements which have at least two nodes, say i and j, on the boundary. Then

$$d_{p,q}^e = (1 + \delta_{pq}) l_{pq}/6, \qquad p, q = i, j \tag{21}$$

where l_{ij} is the distance between the nodes i and j. The contributions to the vectors $[r_p^n]$ and $[s_p^n]$ from e are found to be

$$\left.\begin{aligned} (r_p^n)e &= \left[4f^n + \beta^n \sum_{q=i,j,k} (1 + \delta_{pq}) V_q^n\right] \Delta^e/12 \\ (s_p^n)^e &= \left[\gamma^n \sum_{q=i,j,k} (1 + \delta_{pq}) B_q^n\right] \Delta^e/12 \end{aligned}\right\} \; p = i, j, k \tag{22}$$

The elementwise assembly of the above matrices and vectors can be done by well known methods.[23–26] For the matrices it is to be done only once and used for all time steps. The vectors, however, are to be evaluated after each time step.

NUMERICAL SOLUTION AND DISCUSSION

To solve (17) and (18) we first eliminate V_q^* from (17) and (18) and solve the resulting system for B_q^*. V_q^* is then known from (17). As already mentioned, the coefficient matrices are to be evaluated only once and used for all time steps. The right hand sides, however, are time dependent and evaluated after every time step. Knowing V^* and B^*, the values at time t^{n+1} are known from (12). Since the initial values $t^0 = 0$ are known from the initial conditions, we can proceed step by step in the time direction and evaluate V^n, B^n for $n = 1, 2, 3, \ldots$. As $n \to \infty$, we get the steady state solutions. We have illustrated the procedure by taking pipes of rectangular, circular and triangular cross-sections. Velocity, induced magnetic field and the flux across the section have been evaluated and graphed at various time levels for different values of M and λ.

For all calculations we have chosen $R = R_m = 1$. Also for the transient flow with constant pressure gradient we have $f(t) = 1$. However, for pulsating flows $f(t)$ may be taken as a periodic function of time. In our case, we have assumed that initially the fluid was at rest and then started by applying constant pressure gradient. As $t \to \infty$, we get the steady state solutions on which extensive literature exists particularly for non-conducting walls. So it has been possible to check the accuracy of the result in these special cases. For rectangular and circular pipes with non-conducting walls ($\lambda = \infty$) the steady state exact solutions have been found by Shercliff[1] and Gold.[3] Our results agree with them to roughly three significant digits.

Rectangular pipe

We have taken a square pipe bounded by the lines $x = \pm 1$, $y = \pm 1$. The whole section has been divided into 128 elements with 49 internal nodes and 32 boundary nodes. Figures 1

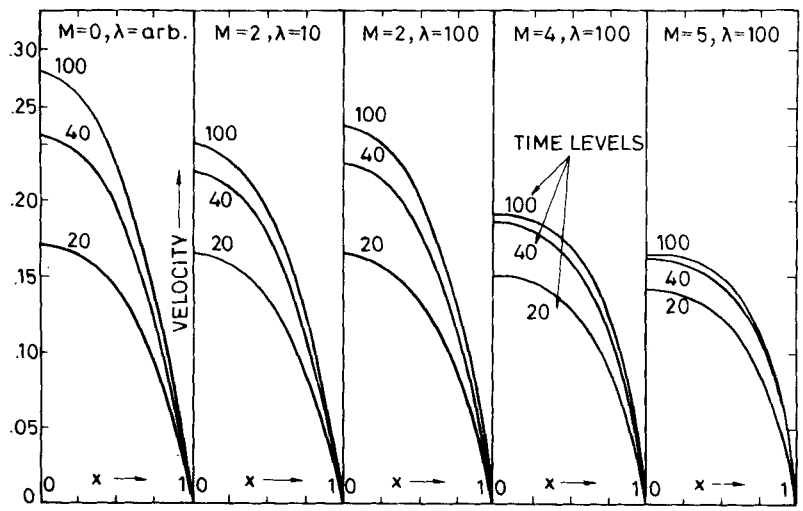

Figure 1. Velocity along $y = 0$, $0 \le x \le 1$ (rectangular pipe)

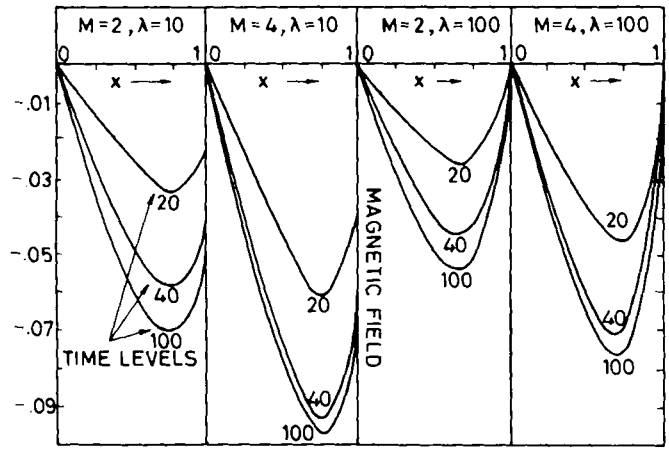

Figure 2. Induced magnetic field along $y = 0, 0 \leq x \leq 1$ (rectangular pipe)

and 2 depict the behaviours of velocity and induced magnetic field along the x-axis ($y = 0, 0 \leq x \leq 1$). Figure 3 gives the flux at different times for various values of M and λ.

Circular pipe

The section $x^2 + y^2 \leq 1$ has been divided into 54 elements with 19 internal nodes and 18 boundary nodes as shown in Figure 4. The mesh generation is done by the method suggested in Reference 25. Figures 5–7 give the velocity and induced magnetic field along the x-axis ($y = 0, 0 \leq x \leq 1$) and the flux across a section for various values of M and λ at different times.

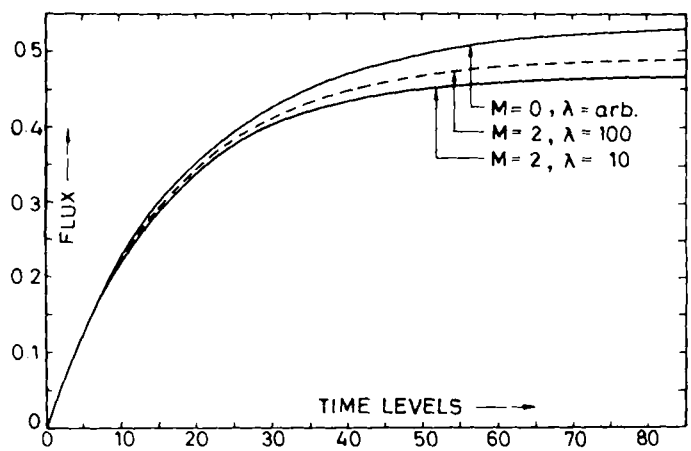

Figure 3. Flux through a section (rectangular pipe)

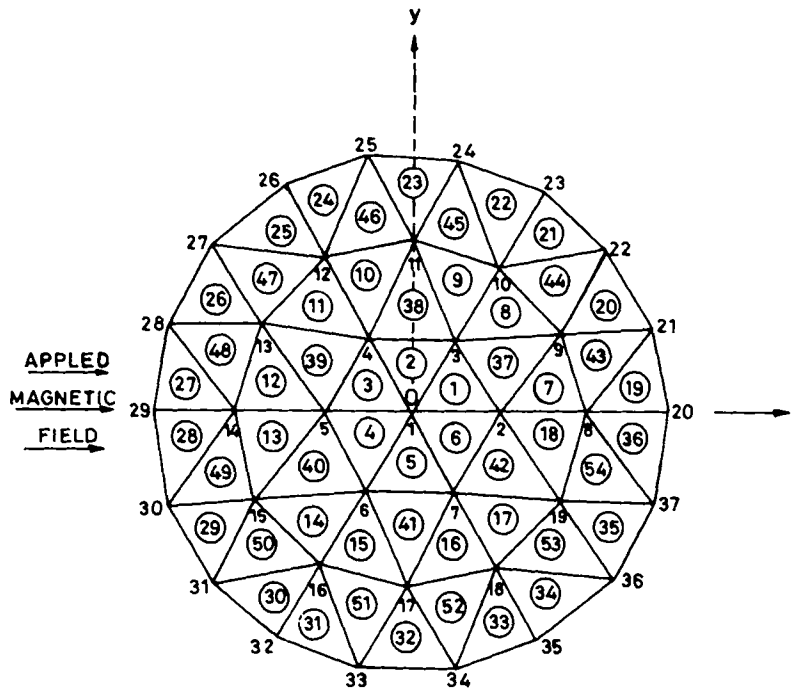

Figure 4. Section of circular pipe

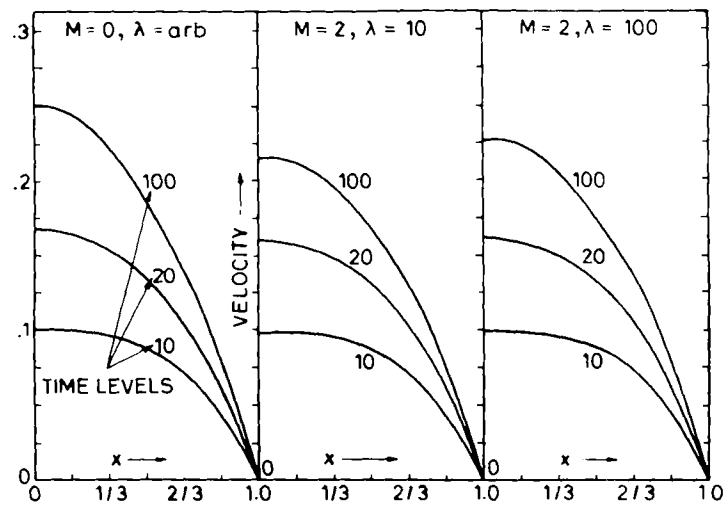

Figure 5. Velocity along $y = 0$, $0 \leq x \leq 1$ (circular pipe)

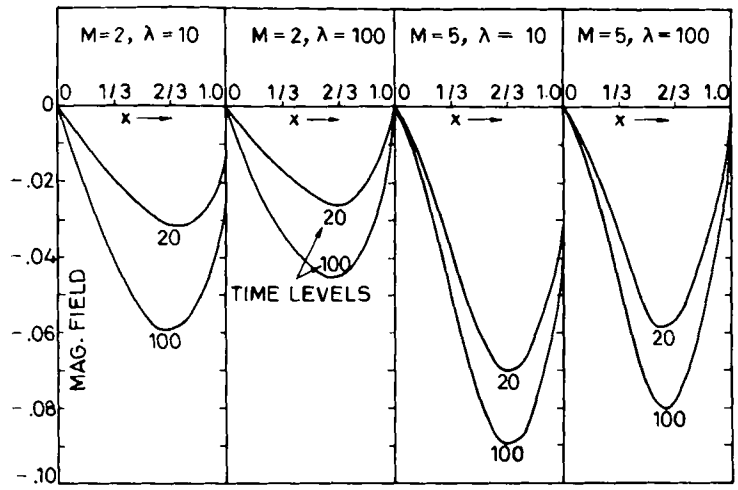

Figure 6. Induced magnetic field along $y = 0$, $0 \leq x \leq 1$ (circular pipe)

Equilateral triangular pipe

We take a section of the pipe bounded by the lines $y = 0$, $y = \pm\sqrt{3}(x \pm 1/2)$. The whole section is divided into 81 elements by lines parallel to the sides. This gives in all 28 internal and 27 boundary nodes. The velocity and induced magnetic field along the line $y = (x + 1/2)/\sqrt{3}$ and the flux across a section are as given in Figures 8–10.

Discussion

From the above results for the pipes of three different cross-sections we make the following observations:

(i) As the Hartmann number increases (keeping λ fixed), the velocity profile shows a

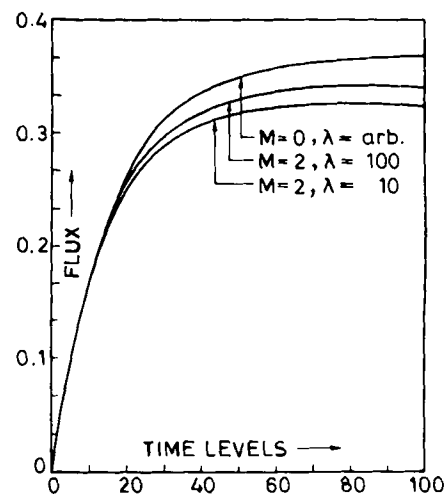

Figure 7. Flux through a section (circular pipe)

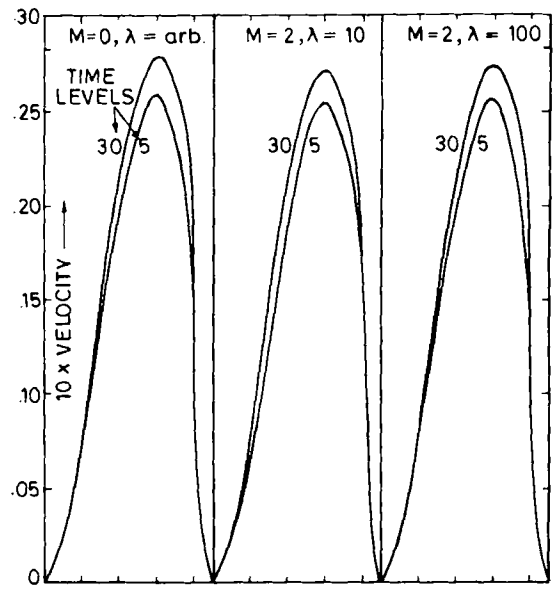

Figure 8. Velocity along $y = (x + 1/2)/\sqrt{3}$ (triangular pipe)

flattening tendency and the net flux across a section decreases. This is a well known characteristic of MHD flows. The magnetic lines of force act like stretched rubber bands which create hindrance to the flow, thereby flattening the velocity profile and reducing the flux. Also with the increase in M, the steady state is approached at a faster rate.

(ii) As the wall conductivity increases or λ decreases (keeping M fixed), the flux decreases. Similar observations have been made in Reference 27 for MHD flows at

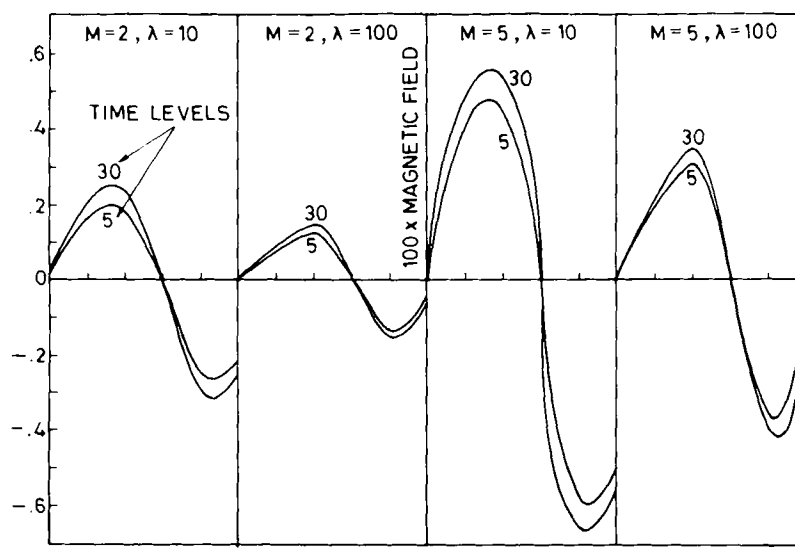

Figure 9. Induced magnetic field along $y = (x + 1/2)/\sqrt{3}$ (triangular pipe)

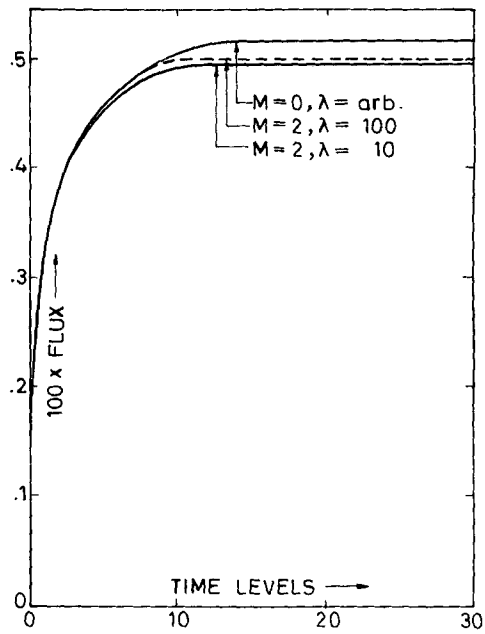

Figure 10. Flux through a section (triangular pipe)

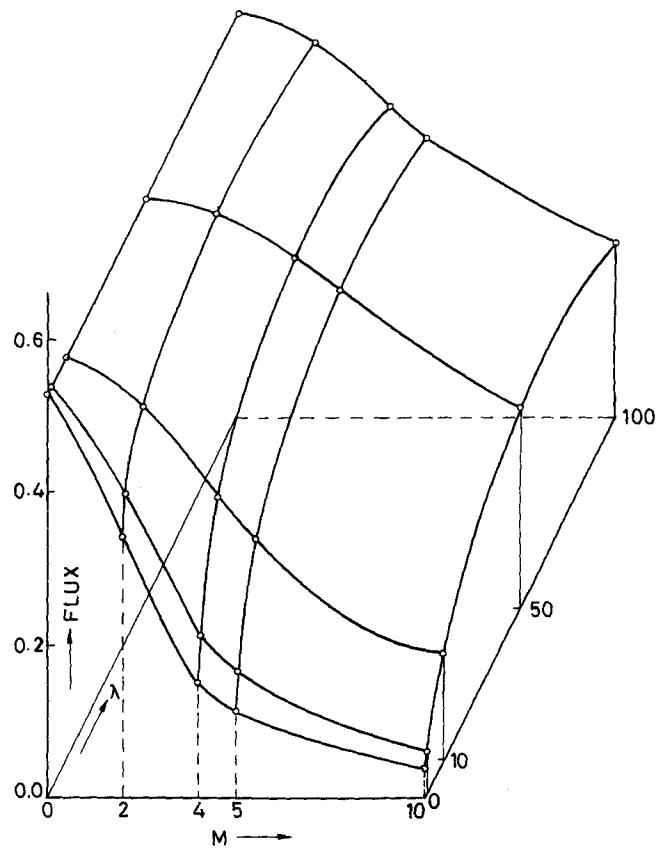

Figure 11. Combined effect of wall conductivity and Hartmann number on flux (rectangular pipe)

high M. The authors have also come to the same conclusion for steady state flows in Reference 14. The explanation of this phenomenon is that as the wall conductivity increases, more and more of the electric currents return through the walls rather than through the fluid itself. So the Lorentz forces tend to oppose the motion in the entire section thereby reducing the flux. This may be of some interest in some prospective thermonuclear reactors in getting lithium through magnetic fields. In a copper pipe the flux will be less than that in a steel pipe.

(iii) The combined effect of Hartmann number and wall conductivity on the flux is shown in Figure 11 for a rectangular pipe at time level 100. The effect at other time levels is the same. As was expected for $M = 0$, wall conductivity has no effect on flow. As either M or wall conductivity increases (or λ decreases) the flux is reduced. The same remains true for pipes of circular and triangular cross-sections.

(iv) Comparing the flux per unit area or the average velocity for the three types of sections described above, we find that the average velocity is maximum for the rectangular pipe, and minimum for the triangular pipe.

REFERENCES

1. J. A. Shercliff, 'Steady motion of conducting fluids in pipes under transverse magnetic fields', *Proc. Camb. Phil. Soc.* **49,** 136–144 (1953).
2. J. A. Shercliff, 'The flow of conducting fluids in circular pipes under transverse magnetic fields', *J. Fluid Mech.*, **I,** (6), 644 (1956).
3. R. R. Gold, 'Magnetohydrodynamic pipe flow I', *J. Fluid Mech.*, **13,** 505 (1962).
4. C. C. Chang and T. S. Lundgren, 'Duct flow in magnetohydrodynamics', *ZAMP*, **12,** 100–114 (1961).
5. J. C. R. Hunt, 'MHD flow in a rectangular duct', *J. Fluid Mech.*, **21,** (4), 577–590 (1965).
6. J. C. R. Hunt and K. Stewartson, 'MHD flow in a rectangular duct II'. *J. Fluid Mech.*, **23,** (3), 563–581 (1965).
7. B. Singh and J. Lal, 'Steady MHD flow through a pipe which has sector as a cross-section under radial magnetic field', Accepted for *Ind. J. Pure Appl. Math.*
8. S. C. Gupta and B. Singh, 'Steady MHD flow through an elliptic pipe', to appear.
9. S. Globe, 'Laminar steady state flow in an annular channel', *Phy. Fluids*, **2,** (4), 404–407 (1959).
10. J. Lal, *Ph.D. Thesis*, University of Roorkee, 1981.
11. B. Singh and J. Lal, 'Magnetohydrodynamic axial flow in a triangular pipe under transverse magnetic field', *Ind. J. Pure Appl. Math.*, **9,** (2), 101–115 (1978).
12. B. Singh and J. Lal, 'MHD axial flow in a triangular pipe under transverse magnetic field parallel to a side of the triangle', *Ind. J. Tech.*, **17,** 184–189 (1979).
13. B. Singh and J. Lal, 'Finite element method in magnetohydrodynamic channel flow problems', *Int. J. Num. Math. Eng.*, **18,** 1091–1111 (1982).
14. B. Singh and J. Lal, 'Finite element method for MHD channel flows with arbitrary wall conductivity', to appear 1982.
15. B. Singh and J. Lal, 'A fast direct method for MHD channel flow through a rectangular pipe'. *Ind. J. Tech.*, **20,** 163–167 (1982).
16. S. C. Gupta and B. Singh, 'Unsteady MHD flow in a circular pipe under transverse magnetic field' *Phy. Fluids*, **13,** (2), 346–352 (1970).
17. S. C. Gupta and B. Singh, 'Unsteady MHD flow in a rectangular channel under transverse magnetic field' *J. Pure Appl. Math.*, **3,** (6), 1038–1047 (1972).
18. R. K. Gupta, 'Unsteady hydromagnetic pipe flow at small Hartmann number', *Appl. Sc. Res.*, **12,** (1), 33–47 (1965).
19. S. C. Gupta and M. L. Mittal, 'Laminar unsteady MHD flow in an annular channel under radial magnetic field', *Appl. Sc. Res. B.*, **11,** (1964).
20. B. Singh and J. Lal, 'Unsteady MHD flow through a rectangular pipe, to appear in *Ind. J. Tech.*
21. S. Y. Wu, 'Unsteady MHD duct flow by finite element method', *Int. J. Nummetr. Eng.*, **6,** 3 (1973).
22. A. Verruijt, 'Solution of transient groundwater flow problems by finite element method', *Water Resources Research*, **8,** (3), 1972).
23. D. H. Norrie and G. de Vries, *An Introduction to Finite Element Analysis*, Academic Press, 1978.
24. G. F. Pinder and M. G. Gray, *Finite Element Simulation in Surface and Subsurface Hydrology*, Academic Press, 1977.
25. R. T. Fenner, *Finite Element Methods for Engineers*, Macmillan 1975.
26. O. C. Zienkiewicz, *The Finite Element Method.* McGraw-Hill, 1977.
27. D. J. Temperley and L. Todd, 'The effects of wall conductivity in MHD duct flows at high Hartmann number', *Proc. Camb. Phil. Soc.*, **69,** 337 (1971).